Inframolecular Protonation Process of *myo*-Inositol 1,4,5-Tris(phosphate) and Related Compounds: Dynamics of the Intramolecular Interactions and Evidence of C−H···O Hydrogen Bonding

Marc Felemez, Philippe Bernard, Gilbert Schlewer, and Bernard Spiess*

Contribution from the Laboratoire de Pharmacochimie Moléculaire, UMR 7081 du CNRS, Faculté de Pharmacie, 74, Route du Rhin, B.P. 24, 67401 Illkirch Cedex, France

Received August 13, 1999. Revised Manuscript Received December 8, 1999

Abstract: The inframolecular protonation process of *myo*-inositol 1,4,5-tris(phosphate) (**1**, Ins(1,4,5)P_3) and the closely related analogues *myo*-inositol 1,4,6-tris(phosphate) (**2**, Ins(1,4,6)P_3), and 3-deoxy-*myo*-inositol 1,4,5-tris(phosphate) (**3**) and the latter's epimer, 3-deoxy-*muco*-inositol 1,4,5-tris(phosphate) (**4**), were explored by performing ^{31}P and ^{1}H NMR titration experiments. The microprotonation scheme for compounds **1**, **2**, and **4** were quantitatively derived. The influence of the configuration of the functional groups and of the presence of the hydroxyls on the ^{31}P and ^{1}H chemical shifts and phosphate basicity was discussed. Thus, the basicity increase of the phosphates and the shielding of the related phosphorus nuclei observed upon deletion of a vicinal hydroxyl is mainly attributed to solvation changes around the phosphate groups. A concerted wrongway shift of some protons and phosphorus nuclei provides information on the conformational dynamics of the phosphates upon protonation. These wrongway shifts may be the result of electrostatic interactions between a ring proton and a doubly negatively charged phosphate group in a trans diequatorial configuration. According to G. R. Desiraju, such an interaction may be considered as a C−H···O hydrogen bond. The necessary condition to observe this bond is a constraint of the phosphate group such that it closely approaches the ring proton. This may occur as shown by molecular modeling studies when two phosphates strongly repel each other either directly or via the relaying effect of an intervening equatorial hydroxyl.

Introduction

(±)D-*myo*-Inositol 1,4,5-tris(phosphate) (**1**, Ins(1,4,5)P_3), arising from the hydrolysis of phosphatidylinositol 4,5-bis(phosphate) in response to many stimuli, plays a crucial role in a wide variety of cellular events.[1−3] Processes such as contraction, secretion, cell proliferation, sensory perception, and neuronal signaling result from a complex spatial and temporal pattern of calcium waves triggered by the binding of Ins(1,4,5)P_3 to its specific receptor.[4−6] The second messenger function of Ins(1,4,5)P_3 is now well established as well as the structural requirements for optimal binding and calcium release activity.[7−11] The synthesis and structure−activity studies of numerous analogues of Ins(1,4,5)P_3 proved that the vicinal 4,5-bis(phosphate) moiety along with the 6-hydroxy motif are essential structural features for the binding to the highly specific Ins(1,4,5)P_3 receptor. However, the events following the Ins(1,4,5)P_3 receptor stimulation are far more complicated than initially thought. In particular, complex mechanisms of regulation involving modulators such as Ca^{2+}, pH, ATP, various proteins, and Ins(1,4,5)P_3 itself control the spatio-temporal characteristics of the Ca^{2+} signaling.[3,7,12−14] Undoubtedly, the receptor, through its binding and coupling domains, is the first target for these modulators, but the ligand also, due to its polyfunctional nature, may be affected. For instance, the sensitive regulation of Ins(1,4,5)P_3 binding in response to intracellular pH alterations may be attributed to the ionization state changes of both the NH_2-terminal ligand binding domain of the receptor and the phosphate groups of the ligand.[15−17] Previous studies of the acid−base properties of Ins(1,4,5)P_3 at an *inframolecular level*, i.e., at each individual phosphate group, confirmed the key role of phosphate P5 in the binding to the receptor, but also evidenced the very peculiar and complex cooperativity between the phosphate groups modulated by the 6-hydroxyl (OH6).[18,19]

(1) Berridge, M. J.; Irvine, R. F. *Nature* **1984**, *312*, 315−321.
(2) Berridge, M. J. *Nature* **1993**, *361*, 315−325.
(3) Berridge, M. J.; Bootman, M. D.; Lipp, P. *Nature* **1998**, *395*, 645−648.
(4) Berridge, M. J. *J. Exp. Biol.* **1997**, *200*, 315−319.
(5) Berridge, M. J. *Ann. N.Y. Acad. Sci.* **1996**, 31−43.
(6) Thomas, A. P.; Bird, G. S. J.; Hajnoczky, G.; Robbgaspers, L. D.; Putney, J. W. *FASEB J.* **1996**, *10*, 1505−1517.
(7) Wilcox, R. A.; Primrose, W. U.; Nahorski, S. R.; Challiss, R. A. J. *Trends Pharmacol. Sci.* **1998**, *19*, 467−475.
(8) Potter, B. V. L.; Lampe, D. *Angew. Chem., Int. Ed. Engl.* **1995**, *34*, 1933−1972.
(9) Wilcox, R. A.; Fauq, A.; Kozikowski, A. P.; Nahorski, S. R. *FEBS Lett.* **1997**, *402*, 241−245.
(10) Wilcox, R. A.; Challiss, R. A. J.; Traynor, J. R.; Fauq, A. H.; Ognayanov, V. I.; Kozikowski, A. P.; Nahorski, S. R. *J. Biol. Chem.* **1994**, *269*, 26815−26821.
(11) Lu, P. J.; Chen, C. S. *Phosphorus Sulfur* **1996**, *110*, 325−328.
(12) Yoshida, Y.; Imai, S. *Jpn. J. Pharmacol.* **1997**, *74*, 125−137.
(13) Taylor, C. W.; Traynor, D. *J. Membr. Biol.* **1995**, *145*, 109−118.
(14) Taylor, C. W. *Trends Pharmacol. Sci.* **1994**, *15*, 271−274.
(15) Guillemette, G.; Segui, J. A. *Mol. Endo.* **1988**, *2* (12), 1249−1255.
(16) O'Rourke, F.; Feinstein, M. B. *Biochem. J.* **1990**, *267*, 297−302.
(17) Worley, P. F.; Baraban, J. M.; Supattapone, S.; Wilson, V. S.; Snyder, S. H. *J. Biol. Chem.* **1987**, *262*, 12132−12136.
(18) Schmitt, L.; Schlewer, G.; Spiess, B. *Biochim. Biophys. Acta* **1991**, *1075*, 139−140.
(19) Guédat, P.; Poitras, M.; Spiess, B.; Guillemette, G.; Schlewer, G. *Bioorg. Med. Chem. Lett.* **1996**, *6*, 1175−1178.

10.1021/ja992940t CCC: $19.00
Published on Web 03/21/2000

Scheme 1

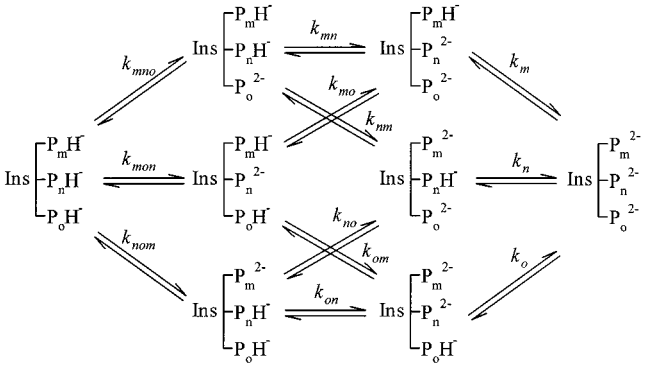

For polyfunctional ligands such as inositol-phosphates the knowledge of the acid−base properties in terms of macroscopic constants provides information about the overall charge of the molecule at any pH which is of great interest in explaining physicochemical, structural, and biological properties of the molecules. However, these macroscopic constants characterize the molecule as a whole and, in the general case where the basicities of the functional groups are not very different, they cannot be assigned to an individual group. Therefore, the consideration and quantification of the acid−base properties at an inframolecular level afford a much better way of analyzing subtle intramolecular interactions which may be one of the key issues in understanding the mechanisms of a biological process. ^{31}P NMR has proved to be a very powerful technique for studying the acid−base behavior of phytic acid, the well-known hexaphosphorylated inositol,[20−22] but more especially in elucidating the intrinsic basicity of each phosphate group for less phosphorylated derivatives. Thus, microscopic constants could recently be derived by our group for bi- and triphosphorylated compounds.[18,23−27] However, an unexpected initial downfield shift of the resonance related to the phosphate in position 1 (P1), occurring at high pH during the first protonation step, prevented, for Ins(1,4,5)P_3, the calculation of microscopic constants. On the basis of only the ^{31}P NMR titration curves, this unusual shift of P1 was tentatively attributed to the formation of a hydrogen bond between the deprotonated P1 and OH2.[18,28] To shed new light on the intimate mechanism of protonation and phosphate conformation changes of Ins(1,4,5)-P_3 we report herein the potentiometric, ^{31}P and ^{1}H NMR titration studies of closely related analogues, i.e., (±)*myo*-inositol 1,4,6-tris(phosphate) (**2**, Ins(1,4,6)P_3), (±)3-deoxy-*myo*-inositol 1,4,5-tris(phosphate) (**3**) and the latter's epimer, and (±)3-deoxy-*muco*-inositol 1,4,5-tris(phosphate) (**4**). Moreover, the microprotonation equilibria scheme (Scheme 1) of *myo*-inositol 1,4,5-tris(phosphate) (**1**) is reconsidered and for the first time quantitatively derived by making suitable approximations of the limiting ^{31}P chemical shifts. The studies were performed in 0.2 M KCl, at 37 °C, near physiological ionic strength and temperature.

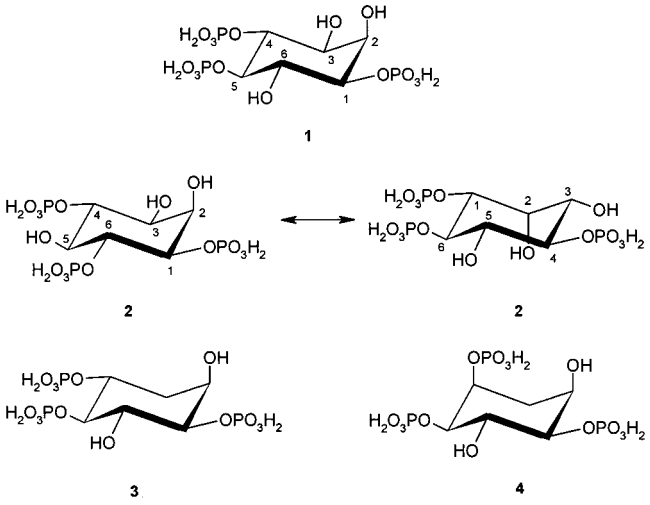

In addition to the NMR titration experiments, conformational and molecular dynamic studies on compound **1** were carried out to link the unusual experimental observations with the computational results.

Experimental Section

Materials. (±)D-*myo*-Inositol 1,4,5-tris(phosphate) and (±)*myo*-inositol 1,4,6-tris(phosphate) were synthesized as previously described.[29] (±)3-Deoxy-*myo*-inositol 1,4,5-tris(phosphate) and its epimer the (±)3-deoxy-*muco*-inositol 1,4,5-tris(phosphate), synthesized and provided by Chapleur et al.,[30] were used without further purification.

Potentiometric Studies and NMR Determinations. Potentiometric and NMR determinations were carried out as previously reported.[23,31] The experiments were performed in two steps in which the same initial solution of the studied compounds of about 4×10^{-3} mol·dm^{-3} was successively subjected to potentiometric and ^{31}P NMR or ^{1}H NMR titrations. The processing of the pH measurements allowed the total concentration of the ligand and the acid as well as the macroscopic protonation constants (by using SUPERQUAD[32]) to be determined. One-dimensional ^{31}P NMR spectra were recorded at 121.50 MHz on a Bruker DPX-300 Fourier transform spectrometer. Field-frequency lock was achieved using 10% $^{2}H_2O$. ^{31}P chemical shift values were referenced to an external 85% H_3PO_4 signal at 0.00 ppm with downfield shifts represented by positive values. Spectra were acquired over a spectral width of 10 ppm using a 0.1 s relaxation delay and a $\pi/2$ pulse. Typically 1K data points were sampled with a corresponding 0.4 s acquisition time. Data were zero-filled and a 1 Hz exponential line broadening function was applied prior to Fourier transformation. The spectra had in general a digital resolution of 1.19 Hz per point. For performing the $^{3}J_{H-P}$ vs pH titration curves, the digital resolution was 0.12 Hz per point. The HypNMR program[33] was used to check the potentiometrically determined protonation constants. The ^{1}H NMR titration was performed on 0.45 mL of solution in $^{2}H_2O$ on the same equipment as before. Spectra were acquired with water presaturation over a spectral width of 6 ppm using a 3 s relaxation delay and a $\pi/2$

(20) Isbrandt, L. R.; Oertel, R. P. *J. Am. Chem. Soc.* **1980**, *102*, 3144−3148.
(21) Brigando, C.; Mossoyan, J. C.; Favier, F.; Benlian, D. J. *Chem. Soc., Dalton Trans.* **1995**, 575−578.
(22) Paton, G.; Noailly, M.; Mossoyan, J. C. *J. Phys. Org. Chem.* **1999**, *12*, 401−407.
(23) Mernissi-Arifi, K.; Schmitt, L.; Schlewer, G.; Spiess, B. *Anal. Chem.* **1995**, *67*, 2567−2574.
(24) Mernissi-Arifi, K.; Ballereau, S.; Schlewer, G.; Spiess, B.; Zenkouar, M. *New J. Chem.* **1996**, *20*, 1087−1092.
(25) Guédat, P.; Schlewer, G.; Krempp, E.; Riley, A. M.; Potter, B. V. L.; Spiess, B. *Chem. Commun.* **1997**, 625−626.
(26) Riley, A. M.; Guedat, P.; Schlewer, G.; Spiess, B.; Potter, B. V. L. *J. Org. Chem.* **1998**, *63*, 295−305.
(27) Mernissi-Arifi, K.; Schlewer, G.; Spiess, B. *Carbohydr. Res.* **1998**, *308*, 9−17.
(28) Schlewer, G.; Guedat, P.; Ballereau, S.; Schmitt, L.; Spiess, B. In *Phosphoinositides: chemistry, biochemistry, and biomedical applications*; Bruzik, K. S., Ed.; American Chemical Society: Washington, DC, 1999; pp 255−270.
(29) Mills, S. J.; Alhafidh, J.; Westwick, J.; Potter, B. V. L. *Bioorg. Med. Chem. Lett.* **1993**, *3*, 2599−2604.
(30) Poirot, E.; Bourdon, H.; Chretien, F.; Chapleur, Y.; Berthon, B.; Hilly, M.; Mauger, J. P.; Guillon, G. *Bioorg. Med. Chem. Lett.* **1995**, *5*, 569−572.
(31) Schmitt, L.; Bortmann, P.; Schlewer, G.; Spiess, B. *J. Chem. Soc., Perkin Trans. 2* **1993**, 2257−2263.
(32) Gans, P.; Sabatini, A.; Vacca, A. *J. Chem. Soc., Dalton Trans.* **1985**, 1195−1200.
(33) Frassineti, C.; Ghelli, S.; Gans, P.; Sabatini, A.; Moruzzi, M. S.; Vacca, A. *Anal. Biochem.* **1995**, *231*, 374−382.

pulse. 4 K data points were sampled with a corresponding 1.14 s acquisition time. The spectra had a digital resolution of 0.44 Hz per point. The temperature in both cases was controlled at 310 ± 0.5 K. The proton and phosphorus resonances of compounds **1** to **4** were assigned by performing proton−proton and phosphorus−proton 2D correlation experiments at two suitable pH values at least, thus allowing the titration curves to be unambiguously characterized.

Computational Methods. The molecular modeling was carried out by using Sybyl 6.5[34] on a Silicon Graphics O_2 R10000 Station. To analyze the conformational changes upon addition of the first proton to Ins(1,4,5)P_3 (**1**), two molecules (forms A and B) were constructed using the Get Fragment option. Forms A and B of compound **1** correspond respectively to the free form and to the P5 protonated form.

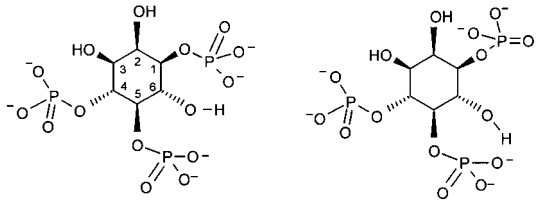

A1 A2

Form A

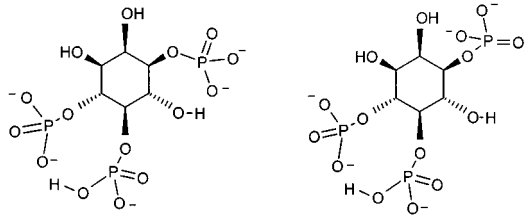

B1 B2

Form B

The starting conformations were optimized by molecular mechanics algorithms operating with the Tripos Force Field. The electrostatic component was applied by means of the Gasteiger-Marsili charges and a dielectric function equal to 1. The lowest energy conformations were found by means of the Sybyl/Systematic Search option. For each form, all rotatable bonds were used and the rotation step was fixed to 10°. Each conformer was minimized as described above. Then, the lowest energy conformations were considered as initial conformations for the molecular dynamic process. The molecular dynamic studies were performed at 300 K starting from a Boltzmann distribution set for a simulation time of 10 ps. The conformations were recorded every 50 fs.

Results and Discussion

Macroscopic and Microscopic Protonation Constants. All the ligands under consideration carry three phosphate groups, each group being able to bind only one proton for pH values ranging from 12 to 3. Thus, the stepwise protonation process can be defined by K_y, characterizing the equilibrium

$$H_{y-1}L^{(7-y)-} + H^+ \overset{K_y}{\leftrightarrows} H_yL^{(6-y)-}$$

These constants can be determined from potentiometric and ^{31}P NMR titration curves by treating the pH or chemical shift data with the program SUPERQUAD[32] or HypNMR,[33] respectively.

Moreover, if the observed chemical shifts for the phosphorus resonances δ_i^{obs} mainly depend on the electronic effects accompanying the variations in the protonation states, then the protonated fraction $f_{i,p}$ of a phosphate group in position i on the inositol ring can be calculated by:

$$f_{i,p} = \frac{\delta_i^{obs} - \delta_{i,d}}{\delta_{i,p} - \delta_{i,d}}$$

where $\delta_{i,p}$ and $\delta_{i,d}$ correspond respectively to the chemical shifts of the protonated and deprotonated fractions of the phosphate in position i.

By summing the protonation fraction curves for a given inositol-phosphate, the mean number of protons bound per molecule at any pH can be calculated ($\bar{p} = f(\text{pH})$). When this curve, as was previously stressed,[23] satisfactorily is superimposed upon the potentiometrically calculated $\bar{p} = f(\text{pH})$ curve, then the individual protonation fractions $f_{i,p}$ are allowed to be expressed as a function of the macro- and microprotonation constants, the latter being easily obtained by nonlinear regression.

Results

***myo*-Inositol 1,4,5-Tris(phosphate) (1).** In previous reports we have already discussed the ^{31}P NMR titration curves for Ins(1,4,5)P_3 shown in Figure 1 with special emphasis on the initial wrongway deshielding of P1 observed upon protonation.[18,28] Here, the term wrongway describes a shift in the opposite direction to that which is expected for the protonation of a phosphate group. Due to this unusual shift, there is an attendant uncertainty in $\delta_{1,d}$ that leads to poor superimposition of both potentiometric and NMR $\bar{p} = f(\text{pH})$ curves which impeded the calculation of the microprotonation equilibrium constants of **1**. However, a closer look to these curves reveals that P1, the less basic phosphate group, only begins to protonate and initiate its upfield shift just before the second equivalent of protons is added. Now, as will be further discussed, the initial downfield shift of P1 is related to the binding of the first equivalent of protons between P4 and P5. Thus, the maximum value reached for δ_i^{obs} should represent a good approximation of $\delta_{1,d}$. By taking this value into account, the protonation fraction curves of Figure 1c and the microprotonation constants listed in Table 1 were obtained. It can be noted that the calculated $f_{i,p}$ curves for P4 and P5 fit the experimental data well and for P1 the fit remains satisfactorily.

The peculiar behavior of the phosphorus titration curves prompted us to perform ^{1}H NMR titration experiments to reveal any observations which could shed light on the mechanism of the protonation process. Usually protonation of a compound leads to downfield shifts in ^{1}H spectra. This is, indeed, observed for all ring protons (Figure 2), excepted for H2 which, to the contrary, moves to higher fields as previously mentioned for some nucleotide protons.[35−39] Interestingly, this H2 proton wrongway shift arises simultaneously with the P1 phosphorus wrongway shift. As expected, the axial protons bound to phosphorylated carbons are downfield shifted relative to the others and appear more affected by pH variations.

Furthermore, some information on the populated rotameric forms of the phosphates is expected from the $^3J_{H-P}$ couplings

(34) SYBYL Molecular Modeling System (v. 6.5), tripos Associates, St. Louis, MO, 1998.

(35) Schweizer, M. P.; Broom, A. D.; Ts'o, P. O. P.; Hollis, D. P. *J. Am. Chem. Soc.* **1968**, *90*, 1042−1055.

(36) Martin, R. B. *Acc. Chem. Res.* **1985**, *18*, 32−38.

(37) Blindauer, C. A.; Holy, A.; Dvorakova, H.; Sigel, H. *J. Chem. Soc., Perkin Trans. 2* **1997**, 2353−2363.

(38) Tribolet, R.; Sigel, H. *Eur. J. Biochem.* **1987**, *163*, 353−363.

(39) Wang, X.; Simpson, J. H.; Nelson, D. J. *J. Inorg. Biochem.* **1995**, *58*, 29−47.

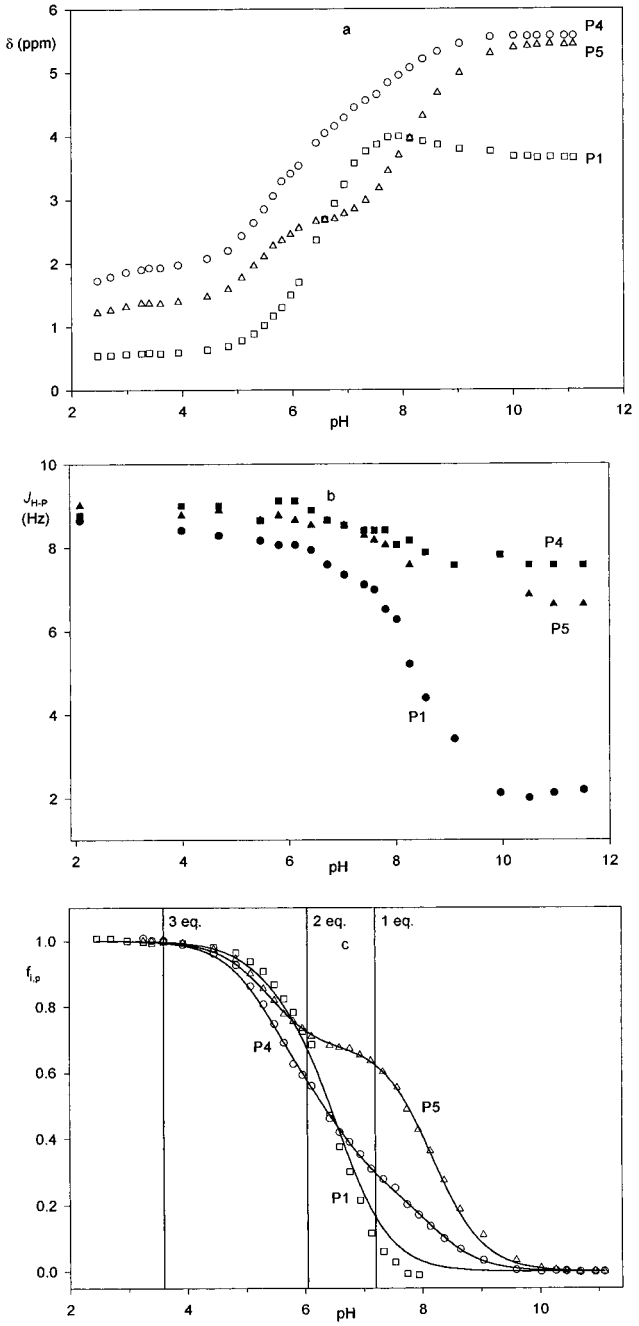

Figure 1. Chemical shifts δ from ^{31}P NMR titrations for Ins(1,4,5)P_3 (**1**) (a), $^3J_{H-P}$ coupling constants (b), and protonation fraction curves $f_{i,p}$ (c) as a function of pH in KCl 0.2 M at 37 °C (10% D_2O). The least-squares fit of $f_{i,p}$ vs pH is shown as a solid line in panel c. The vertical lines correspond to the theoretical addition of 1−3 equiv of protons.

which are related, through the Karplus/Altona equation, to the H−C−O−P dihedral angles.[40] According to this equation, free rotation of a phosphate group would amount to a coupling of 9.3 Hz. Figure 1b, which reports the $^3J_{H-P}$ coupling constants vs pH for the three phosphate groups, shows above pH 5 small deviations from this value for P4 and P5, but marked differences for P1. Noteworthy is that the $^3J_{H1-P1}$ vs pH curve remarkably parallels the P5 protonation fraction curve above pH 6, i.e., in the pH range for which compound **1** carries one or two protons.

***myo*-Inositol 1,4,6-Tris(phosphate) (2).** As depicted above, it can be seen that Ins(1,4,6)P_3 retains the minimal structural requirements for partial agonism at the Ins(1,4,5)P_3 receptor. Specifically, the vicinal bis(phosphate) moiety of **1** corresponds to P1 and P6 of **2**. The additional phosphate group at P4 of **2** is equivalent to P1 of Ins(1,4,5)P_3 and the OH5 hydroxyl group of **2** plays the crucial OH6 role of the natural second messenger **1**. The changes reside in OH2 and OH3 of Ins(1,4,6)P_3, which display inverted configurations with regard to Ins(1,4,5)P_3. Figure 3 shows the ^{31}P NMR titration curves and the corresponding protonation fractions of Ins(1,4,6)P_3. For the purpose of comparison, the δ_i^{obs} vs pH curves of Ins(1,4,5)P_3 are superimposed in a solid line on Figure 3a. It clearly appears that P6 of compound **2** keeps the same biphasic shape and roughly the same $\delta_{i,p}$ and $\delta_{i,d}$ values as P5 in **1**. On the contrary, with regard to **1**, $\delta_{4,p}$ and $\delta_{4,d}$ of **2** are downfield shifted by 1.31 and 1.55 ppm, respectively, whereas $\delta_{1,p}$ and $\delta_{1,d}$ are upfield shifted by 1.00 and 1.49 ppm. In addition, the wrongway deshielding of P1 in **1** upon initial protonation is no longer observed for P4 in **2**. The macroscopic as well as microscopic protonation constants are listed in Table 1. It can be noted that there is good agreement between the potentiometric and the NMR determined macroprotonation constants. The ^{1}H NMR titration curves of **2** shown in Figure 4 exhibit some differences from those of **1**. The protons H6 and H5 are respectively upfield and downfield shifted by about 0.28 ppm relative to H5 and H6 of **1** even though they experience the same chemical environment. H1 and H4 of **2**, which correspond to H4 and H1 of **1**, are both axially orientated but in **2** the neighboring hydroxyl is inverted. Thus, by comparing H1 of **1** with H4 of **2** and H1 of **2** with H4 of **1**, it can be observed that the protons are deshielded by about 0.20 ppm on going from a cis to a trans antiperiplanar configuration. Finally, H2 and H3, in reverse configuration when comparing **2** to **1**, undergo the largest shift since the change from an equatorial to an axial position results in an upfield shift of about 0.53 ppm. This observation concerns the acidic part of the titration curves rather than the basic part, for which H2 of **2** again shows a very marked wrongway shift. It is noteworthy that H2, upon protonation of **2**, first moves highfield in a biphasic manner before taking the "right way" downfield.

3-Deoxy-*myo*-inositol 1,4,5-Tris(phosphate) (3). 3-Deoxy-*myo*-inositol 1,4,5-tris(phosphate) (**3**) is among the studied molecules the only compound having its functional groups in the same configuration as **1**, differing from the latter by the deletion of OH3. However, even though OH3 is not considered as critical as OH6 for calcium release and binding to the Ins(1,4,5)P_3 receptor, there is about a 10-fold decrease in affinity for **3** with regard to **1**.[30] ^{31}P and ^{1}H NMR titrations were thus performed to detect any changes in the physicochemical parameters of **3** with regard to **1**. These titration curves are respectively reported in Figures 5 and 6. Unfortunately, the presence of minor impurities prevented the determination of the microprotonation constants. Nevertheless, the examination of these curves shows that small structural changes may be evidenced by noticeable spectral variations. In the phosphorus NMR titration curves the effect of the OH3 deletion on $\delta_{i,p}$ and $\delta_{i,d}$ of the phosphate groups can be observed. The magnitude of the changes in chemical shifts decreases in the following order: P4 ≫ P5 > P1. Since the effect on P4 is expected, the difference in behavior in P5 and P1 is more surprising as both phosphates are symmetrically located with regard to the C3 position. Also, the superimposition of the $f_{i,p}$ curves for **1** and **3** (curves not shown) reveals an important downfield shift at pH >7 for P4 and P5 of **3**, whereas for both compounds the $f_{1,p}$ vs pH curves are very close. This indicates that the two vicinal

(40) Lankhorst, P. P.; Haasnoot, C. A. G.; Erkelens, C.; Altona, C. J. *Biomol. Struct. Dyn.* **1984**, *1*, 1387−1405.

Table 1. Logarithms of the Macro- and Microprotonation Constants for the Studied Compounds

ligand	*y*	log K_y	*i*	log k_i	*ii′*	log $k_{ii'}$	*ii′i″*	log $k_{ii'i''}$
Ins (1,4,5)P_3 (**1**)	1	8.18 (0.02)	*1*	6.49 (0.02)	*14*	7.87 (0.02)	*145*	5.87 (0.09)
	2	6.61 (0.02)	*4*	7.58 (0.02)	*15*	7.90 (0.01)	*154*	5.82 (0.08)
	3	5.39 (0.04)	*5*	8.01 (0.01)	*41*	6.66 (0.04)	*541*	5.90 (0.08)
					45	6.66 (0.04)		
					51	6.32 (0.02)		
					54	6.31 (0.02)		
Ins(1,4,6)P_3 (**2**)	1	8.17 (0.02)	*1*	7.66 (0.04)	*14*	6.03 (0.04)	*146*	5.80 (0.22)
		8.02 (0.01)	*4*	6.13 (0.02)	*16*	6.28 (0.02)	*164*	5.64 (0.20)
	2	6.09 (0.04)	*6*	8.02 (0.01)	*41*	7.70 (0.01)	*641*	5.69 (0.18)
		6.18 (0.01)			*46*	7.70 (0.01)		
	3	5.21 (0.08)			*61*	5.88 (0.03)		
		5.31(0.01)			*64*	5.88 (0.03)		
deoxy-3-Ins(1,4,5)P_3 (**3**)	1	*8.35 (0.03)*						
	2	*6.68 (0.03)*						
	3	*5.78 (0.04)*						
deoxy-3-muco(1,4,5)P (**4**)	1	8.48 (0.02)	*1*	6.67 (0.01)	*14*	7.94 (0.01)	*145*	6.05 (0.09)
		8.37 (0.04)	*4*	7.82 (0.01)	*15*	7.94 (0.01)	*154*	5.93 (0.09)
	2	6.60 (0.02)	*5*	8.31 (0.01)	*41*	6.63 (0.04)	*541*	5.97 (0.12)
		6.75 (0.05)			*45*	6.78 (0.02)		
	3	5.50 (0.03)			*51*	6.39 (0.02)		
		5.67 (0.06)			*54*	6.29 (0.03)		

[a] The potentiometrically determined macroprotonation constants are given in italics. log k_i, log $k_{ii'}$, and log $k_{ii'i''}$ represent a general designation for respectively the logarithms of the first, second, and third stepwise microprotonation constants. [b] The uncertainties are estimates of the standard deviation as calculated by HypNMR[33] and SUPERQUAD[32] for the macroprotonation constants and by SIGMAPLOT for the microprotonation constants.

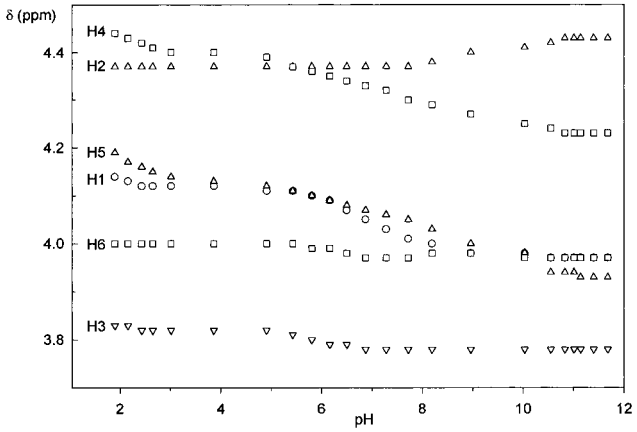

Figure 2. Chemical shifts δ from a ^{1}H NMR titration for **1** as a function of pH in 0.2 M KCl at 37 °C (D_2O).

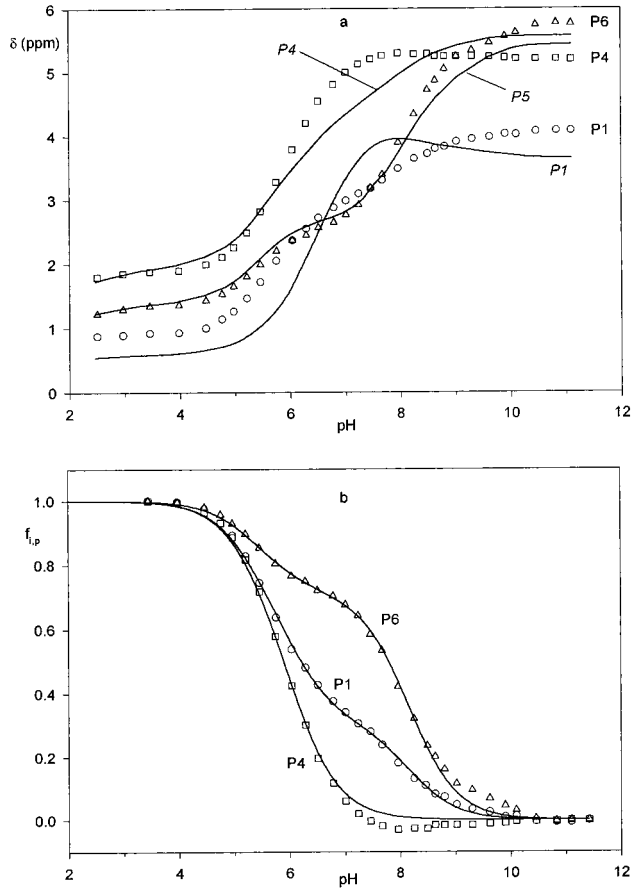

Figure 3. Chemical shifts δ from ^{31}P NMR titrations for Ins(1,4,6)P_3 (**2**) (a) and the corresponding protonation fraction curves $f_{i,p}$ (b) as a function of pH in KCl 0.2 M at 37 °C (10% D_2O). For purpose of comparison the $\delta_i^{obs} = f(pH)$ for Ins(1,4,5)P_3 (**1**) are superimposed in panel a (solid line). The least-squares fit of $f_{i,p}$ vs pH is shown as a solid line in panel b.

phosphates of **3** are more basic than the corresponding phosphates of **1**. The potentiometrically determined protonation constants (Table 1) macroscopically reflect such a basicity increase. Figure 6 displays the ^{1}H NMR titration curves of **3**, which, with the exception of H3, do not show marked differences with those of **1**. Interestingly, in the case of **3**, the effect of the protonation of a phosphate group on the two neighboring axial (ax) and equatorial (eq) protons can be seen. From these curves it appears that H3ax for **1** and **3** are remarkably parallel, with a highfield gap of about 2.08 ppm for **3** relative to **1**. On the contrary, H3eq takes a triphasic shape including, upon protonation, a first diphasic highfield shift followed by a final deshielding. It can be noted that this curve resembles those of H2 of compounds **1** to **3**.

3-Deoxy-*muco*-inositol 1,4,5-Tris(phosphate) (4). Compound **4**, the epimer of **3**, differs from the natural messenger and its analogues by the axial orientation of P4. At first glance, the ^{31}P NMR titration curves (Figure 7) of **4** and **3** look alike, differing only in the shielding of P4 and P5, which is more pronounced when compared to **1**. However, a significant difference appears in that P1 is rigorously monophasic and that the phosphorus wrongway shift is no longer observed. Table 1 contains the macro- and microprotonation constants of **4** which are only slightly higher than those of **1**. In the ^{1}H NMR spectra of the *muco* derivative, the proton resonances are either badly

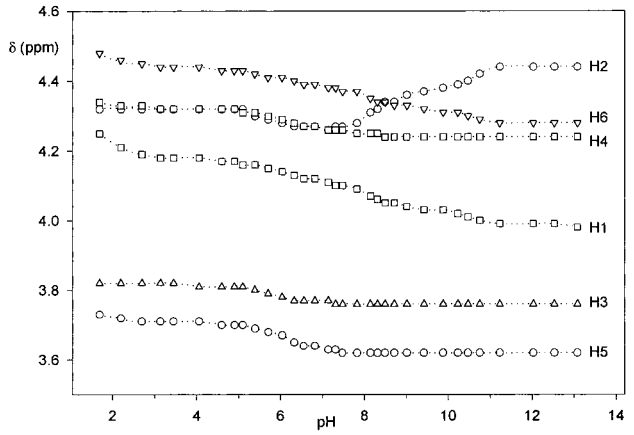

Figure 4. Chemical shifts δ from a ^{1}H NMR titration for **2** as a function of pH in 0.2 M KCl at 37 °C (D_2O).

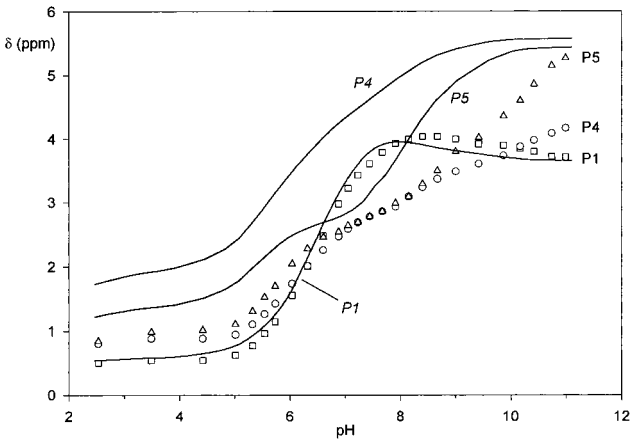

Figure 5. Chemical shifts δ from ^{31}P NMR titrations for deoxy-3 Ins-(1,4,5)P_3 (**3**) as a function of pH in KCl 0.2 M at 37 °C (10% D_2O).

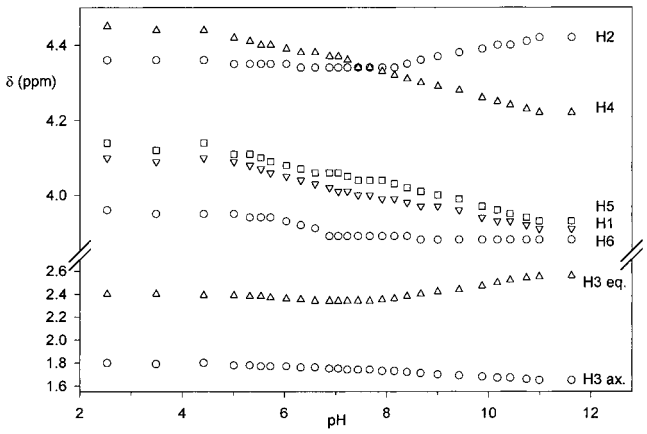

Figure 6. Chemical shifts δ from a ^{1}H NMR titration for **3** as a function of pH in 0.2 M KCl at 37 °C (D_2O).

resolved or perturbed by the H_2O signal. However, it is possible to follow the most downfield and upfield shifted signals H4, H2 and H3ax, H3eq respectively as a function of pH (Figure 8). As for **3**, H3ax is shifted 1.97 ppm upfield compared to H3 of **1** and H3eq shows the same wrongway shift without the shift inversion observed from pH 6.5 to 5. It is noteworthy that, contrary to all the other equatorial protons of the compounds studied, H2 behaves in a manner analogous to all axial protons vicinal to a phosphate group. This shows that the proton wrongway shift earlier mentioned[41] is not an intrinsic property of an equatorial ring proton influenced by the electron-withdrawing effect of a phosphoryl group upon protonation.

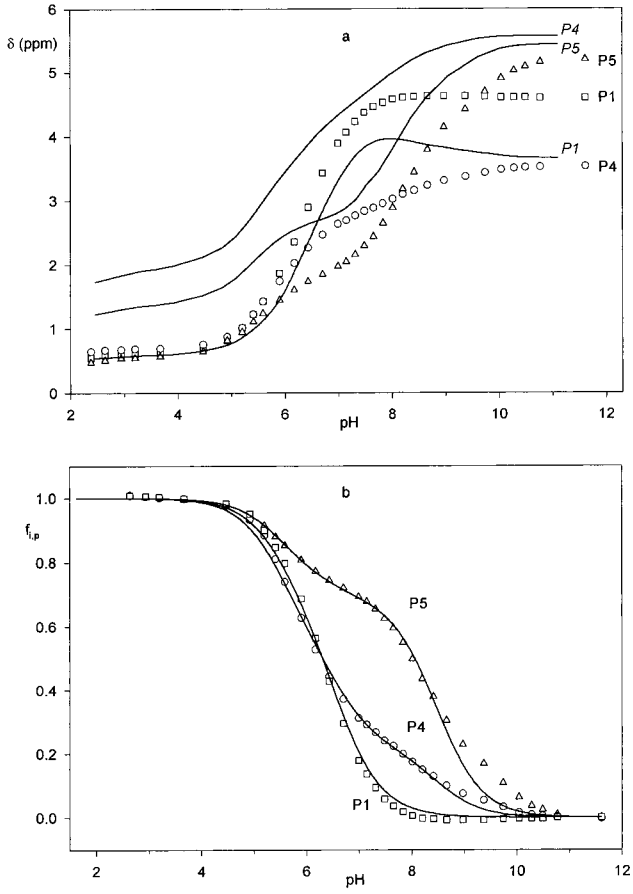

Figure 7. Chemical shifts δ from ^{31}P NMR titrations for deoxy-3 *muco*(1,4,5)P_3 (**4**) (a) and the corresponding protonation fraction curves $f_{i,p}$ (b) as a function of pH in KCl 0.2 M at 37 °C (10% D_2O). For the purpose of comparison the $\delta_i^{obs} = f(\text{pH})$ of Ins(1,4,5)P_3 (**1**) are superimposed in panel a (solid line). The least-squares fit of $f_{i,p}$ vs pH is shown as a solid line in panel b.

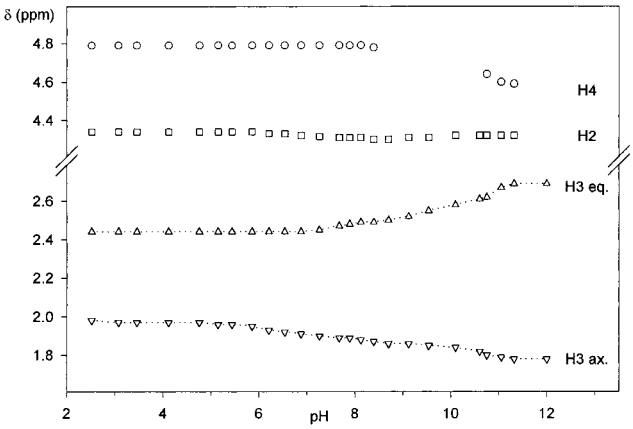

Figure 8. Chemical shifts δ from a ^{1}H NMR titration of the H2 and H4 protons for deoxy-3 *muco*(1,4,5)P_3 (**4**) as a function of pH in 0.2 M KCl at 37 °C (D_2O).

Computational Results. The conformational analysis of Ins-(1,4,5)P_3 reveals for the proton free form (form A) a marked repulsion of the two adjacent P4 and P5 phosphates, whereas in the monoprotonated form (form B) both phosphates are held together by a hydrogen bond. In these conformations, the nearest oxygen atoms of the P4 and P5 phosphates are at a

(41) White, A. M.; Varney, M. A.; Watson, S. P.; Rigby, S.; Changsheng, L.; Ward, J. G.; Reese, C. B.; Graham, H. C.; Williams, R. J. P. *Biochem. J.* **1991**, *278*, 759−764.

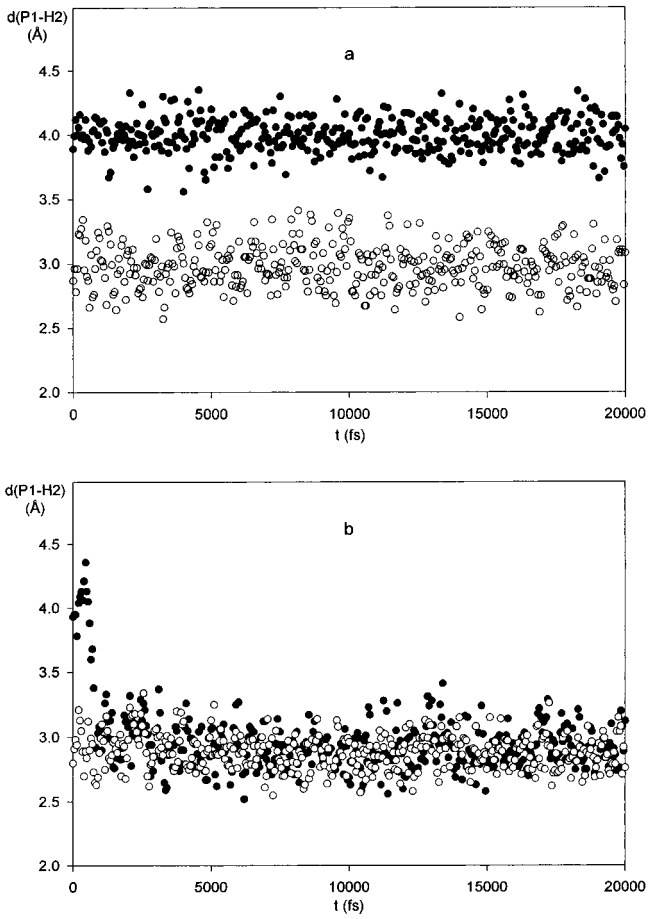

Figure 9. Dynamic (20 ps) of phosphate P1 measured by the P1−H2 distance for (a) conformers B1 (●) and B2 (○) and (b) conformers A1 (●) and A (○).

distance of 6.5 and 2.77 Å in forms A and B, respectively. The repulsion observed in form A leads to the stabilization of the molecule by the formation of two hydrogen bonds between OH3 and an oxygen atom of P4 as well as between OH6 and an oxygen atom of P5. Such a conformation contributes to move P1 close to H2 so that the C−H $\cdots^{2-}O_3P-O$ distance can take a minimum value of 2.5 Å. Some other conformations for P1, lacking interactions, can be found in form A but with at least 3 kcal·mol^{-1} higher energies. On form B, on the contrary, both vicinal phosphates are close together, setting free OH6 which is therefore able to interact with phosphate P1. Thus, two main conformations of equivalent energy are found for phosphate P1 in this form, having P1 orientated either toward OH6 (conformer B1) or toward H2 (conformer B2).

The dynamic process applied on the minimized conformations was followed by considering the distance between the phosphorus atoms of P4 and P5. The results confirm the conformational analysis showing that both vicinal phosphates remain distant in form A and stay in close proximity in form B maintaining during the whole simulation an average distance of 5.7 (min. 5.26 Å, max. 6.23 Å) and 4.6 Å (min. 4.03 Å, max. 5.16 Å), respectively. In the former case a hydrogen bond is formed between an oxygen atom of P5 and OH6 while in the latter case P4 and P5 phosphates interact via the bound proton. The dynamic was also followed by measuring the distance between the phosphorus atom of P1 and H2. For form B, both starting conformations retained in the conformational analysis remain stable and are preserved over the simulation (see Figure 9a). In addition, no significant energy difference is noticed between conformers B1 and B2, indicating that both

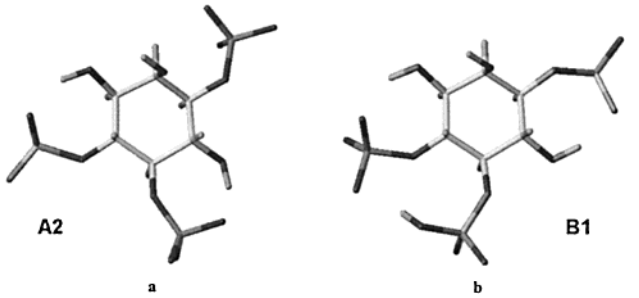

Figure 10. Optimized A2 and B1 conformers.

conformers are likely to occur. The P1−H2 distances are 3.93 (min 3.76 Å, max. 4.35 Å) and 2.97 Å (min. 2.60 Å, max. 3.38 Å) for conformers B1 and B2, respectively. For form A, although the conformational analysis revealed only one possible conformation for the P1 phosphate (this with P1 in the vicinity of H2), conformations A1 and A2 analogous to B1 and B2 were tested. Figure 9b summarizing the analysis shows that only conformer A2 in which P1 is orientated toward H2 is stable allowing a close approach of P1 and H2. On the contrary, conformer A1 rapidly converts into the A2 form confirming the conformational analysis. In the latter form, the average distance of the phosphorus atom of P1 and H2 is 2.90 Å with values of about 120° for the C2−H2−O(P1) angle and 80° for the H2−O(P1)−P1 angle. Optimized structures of conformers A2 and B1 are represented in Figure 10.

Noteworthy is also the hydrogen bond between OH6 and an oxygen atom of P5 which forms in the case of conformer A2 of the deprotonated molecule. As shown in Figure 11, setting of this bond follows the rotation of OH6 at about 9000 ps bringing P5 close to it, which results in a 10 kcal·mol^{-1} gain of energy for the molecule.

Finally, Figure 12 depicts the dynamic of the phosphate groups of the fully deprotonated molecule (form A). In this figure it can be observed after the energetic stabilization of the system that, if the distance of the P4−P5 phosphorus atoms is allowed to shorten, the P1−H2 distance markedly increases, affording for P1 a much larger conformational space (Figure 12, panels a and b). Furthermore, the shortest P4−P5 distances tend to correspond to high energy values (Figure 12, panels a and c), thus indicating that large P1−H2 distances destabilize the molecule by increasing its energy.

Discussion

Structural Influence on the Phosphorus and Proton Chemical Shifts. Clearly the modifications of the hydroxyls play a most important role on the ^{31}P and ^{1}H chemical shift variations since, for instance, the phosphorus resonances move upfield by 1.34 ± 0.20 ppm by deleting such an OH group, or simply by inverting it from an equatorial to an axial position. These modifications also deeply affect the basicity of the phosphates. Thus, the macroprotonation constants are higher for the deoxy derivatives **3** and **4** than for the inositol compounds **1** and **2**. There is, in addition, a significant decrease in the basicity of a phosphate group when the vicinal hydroxyl moves from an axial to an equatorial configuration, as can be noticed in the comparison of log k_1 and log k_4 of **1** and **2**, respectively. With nucleotide-type structures, the OH group was presumed to act either through changes of the solvation shell in the vicinity of the phosphates, via hydrogen bonding, or via electron-inductive effects through σ bonds or through space.[42,43] For the inositol-phosphates and related compounds, the latter reason was

(42) Massoud, S. S.; Sigel, H. *Inorg. Chem.* **1988**, *27*, 1447−1453.

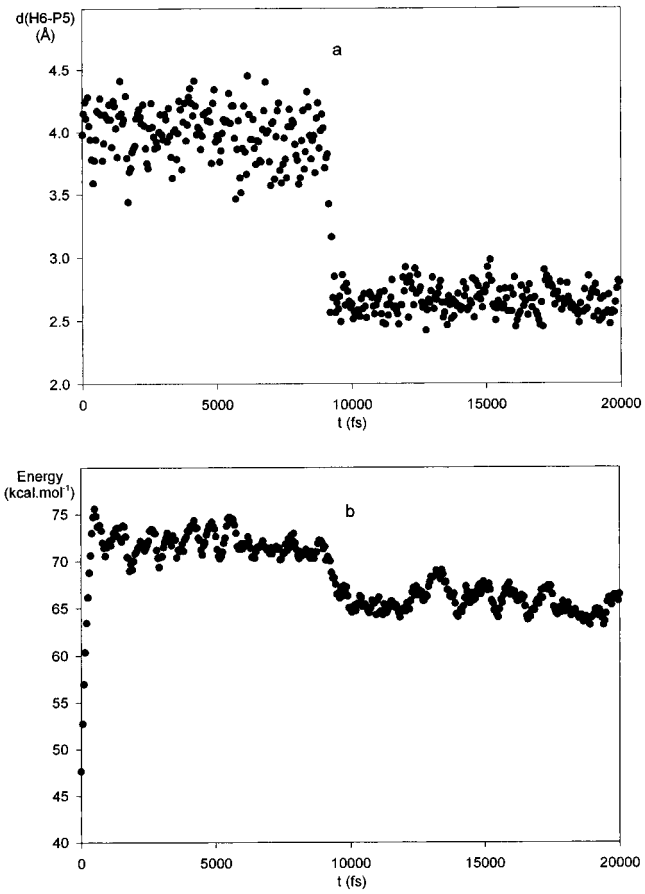

Figure 11. Dynamic (20 ps) of the hydrogen atom of OH6 measured by its distance from the phosphorus atom of P5 for conformer A (a). Total energy variations (b).

discarded since the replacement of an OH group by one or even two fluorine atoms leads to a basicity increase of the neighboring phosphate which is opposite in effect to that expected for an inductive effect.[28] Also, if only such an effect would occur, the influence of the hydroxyl orientation should not be significant and the basicity of P1 and P4 of **1** and **2**, respectively, should be closer than observed. Since coordination of water molecules to the functional groups[44] or even C−H groups[45,46] of many biological molecules seems to be crucial in keeping their structural integrity, it is therefore likely that changes on the hydroxyl groups may deeply affect the hydrogen bonding cooperative interactions of the water molecules and thus lead to noticeable spectral changes for the closest nuclei. The involvement of water molecules around polar groups may also account for the basicity increase of the phosphates accompanying the deletion of an hydroxyl.

Magnitude of the ^{31}P and ^{1}H Chemical Shift Variations vs pH: Observation of a Concerted Wrongway Shift of Both Nuclei. By considering the ^{31}P NMR titration curves of the compounds under study, certain unusual features appeared which provide, in addition to the individual protonation process, an insight into its dynamics. It should be noted that in the following discussion, only the first protonation step of each phosphate group will be considered since the second protonation occurs

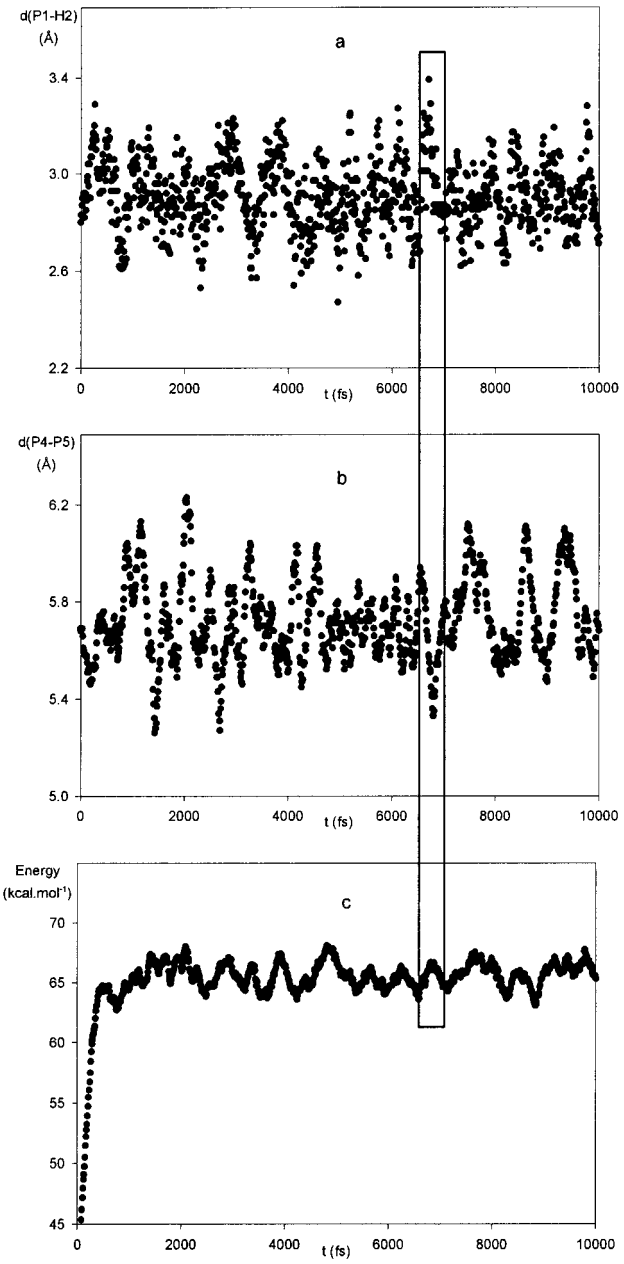

Figure 12. Dynamic of the phosphate groups for conformer A2: (a) dynamic of P1 measured by the P1−H2 distance, (b) relative dynamic of P4 and P5 measured by the phosphorus atoms distance of P4 and P5, and (c) total energy variations.

only for pH values below 2.5. It has been widely observed that, upon protonation, the chemical shifts of the phosphorus nuclei of phosphate groups of various molecules move upfield by several ppm.[23,28,41,43,47,48] Here a clear distinction may be made between phosphates P5, P6 and phosphates P1, P4. The former two phosphates, which generally have two neighboring equatorial functional groups, undergo an upfield shift of 4.3 ± 0.2 ppm. The P1 and P4 phosphates, most often vicinal to an axial hydroxyl or to a deoxy position, experience a shielding of only 3.3 ± 0.3 ppm. Among the latter phosphates, the initial downfield shift found for P1 of **1** and **3** may be responsible for the low $\Delta\delta = \delta_{i,d} - \delta_{i,p}$ values. In P1 of **2** and P4 of **3** and **4**, this downfield shift, although not positively present, is distinguishable in the shape of their titration curves.

(43) Cozzone, P. J.; Jardetzky, O. *Biochemistry* **1976**, *15* (22), 4853−4859.
(44) Bera, A. K.; Mukhopadhyay, B. P.; Pal, A. K.; Haldar, U.; Bhattacharya, S.; Banerjee, A. *J. Chem. Crystallogr.* **1998**, *28*, 509−516.
(45) Jeffrey, G. A. *J. Mol. Struct.* **1994**, *322*, 21−25.
(46) Auffinger, P.; Louise-May, S.; Westhof, E. *Faraday Discuss.* **1996**, *103*, 151−173.
(47) Moerdritzer, K. *Inorg. Chem.* **1967**, *6*, 936−939.
(48) Ollig, J.; Hagele, G. *Comput. Chem.* **1995**, *19*, 287−294.

Protonation of a compound usually leads to downfield shifts of ^{1}H NMR spectra. Thus, on the titration curves performed in this study, a chemical shift difference $\Delta\delta$ of -0.18 ± 0.04 ppm is observed for the protons of the phosphorylated positions owing to the electron-withdrawing effect of the phosphoryl groups. However, the protons bound to non-phosphorylated carbons are also affected by the protonation states of phosphates on the neighboring carbons. For adjacent protons, $\Delta\delta$ is, in general, one-fourth to one-third the value of that of a proton directly bound to a phosphate bearing carbon. In addition to the aforementioned effects, a very unexpected upfield shift, previously termed wrongway shift, can be noticed for some protons that reaches, for instance, 0.26 ppm for H3eq of **4**. The multicomponent and atypical character of these curves prevent the calculation of individual protonation constants but provide information on the dynamics of the protonation process.

The most striking feature of some ^{1}H and ^{31}P NMR titration curves, the shift in the opposite direction to that which is expected upon protonation, warrants further discussion. A ^{1}H wrongway shift has been observed before for H8 of purine nucleoside 5′-monophosphates[35−38] tentatively attributed to either the paramagnetic effect of the anisotropy of the phosphate group or to the direct electrostatic field effect of the negatively charged phosphate. The inositol-phosphates studied in the present work are structurally distant from the nucleotides for which a wrongway shift was first described. A. M. White et al.[41] earlier mentioned the displacement of H2 in the opposite direction to the other resonances for compound **1**, but found such a behavior consistent with the equatorial location of this proton. A close look at our results shows that, indeed, the wrongway shift mainly involves equatorial protons but some exceptions noted for the compounds under study, or other inositol-phosphates, indicate that this is not a necessary condition. Thus, the equatorial H4 of **4** is deshielded upon protonation by 0.2 ppm as for other axial protons, and H2 is only slightly affected. Also H2 of Ins(4,5)P_2 or of Ins(1,2,6)P_3 (unpublished results) move in the expected direction. On the contrary, the axial H4 proton of the latter undergoes a 0.06 ppm wrongway shift. Therefore, other explanations should exist to account for these observations.

Remarkably and never so far observed, the proton wrongway shift may in some cases be concomitant with the initial downfield shift of the vicinal phosphate as exemplified for H2 and P1 of **1** and **3**. This downfield contribution in the phosphorus shift always exists but sometimes appears only through the low $\Delta\delta$ values ($\Delta\delta = 3.3$ ppm instead of 4.3 ppm). At this stage it may be necessary to make clear what we refer to as the ^{31}P wrongway shift, since this phenomenon has never been reported for phosphate groups. As previously mentioned, variation of chemical shift affected by decreasing pH generally results in the expected highfield direction for most phosphate groups. An opposite trend is observed either at the highest pHs as for P1 of **1** and **3** or in the course of a titration for a phosphate between two neighboring phosphate groups. Two examples of such curves are found for P5 of Ins(4,5,6)P_3 or P4 of Ins(1,3,4,5)-P_4.[25,28,49] In the latter case, the unusual deshielding arises from a transfer of protons from the central to the lateral phosphates and is indicative of a deprotonation process even though this deprotonation occurs while the pH decreases. Thus, the observed shift takes the "right way". By contrast, in the former case, P1 of **1** or **3** is deshielded in a pH range where the phosphate remains almost fully deprotonated. The chemical shift variations are due to a phenomenon which differs from a simple proton exchange with the medium and which operates in the opposite direction to that expected according to the pH variations. The same phenomenon is still present when the $\Delta\delta$ values are close to 3 ppm. The curves keep a positive slope over the entire titration only because the rightway shift surpasses the wrongway shift.

For the 5′-purine mononucleotides, the H8 shielding parallels the protonation of the dianionic phosphate group, whereas for **1** and **3**, the H2 shielding occurs while the P1 phosphate keeps almost its fully deprotonated state. This major difference suggests subtle conformational changes of the phosphate groups due to the modulation of the electrostatic interactions between these groups when their charge varies with pH. Thus, these conformational changes may be described as below. At high pH, in the fully deprotonated form of **1** and **3**, P4 and P5 repel each other, so that P1 is constrained toward H2. Subsequently, as the first added proton is simultaneously taken and stabilized by the two vicinal phosphates, the constraint on P1 becomes weaker allowing it to rotate more freely around the C−O bond and permitting easier access to OH6. In that process, the latter hydroxyl group appears crucial in communicating the electrostatic interaction between P5 and P1. The above-described process is also clearly depicted by the variations of the $^3J_{H1-P1}$ coupling constant versus pH of **1** (Figure 2b).[31,50] It is well demonstrated that the relationship between dihedral angles and vicinal couplings follows a Karplus/Altona type equation[40] with $J_{180°} \approx 23$ Hz, $J_{60°} \approx 2.4$ Hz, and $J_{0°} \approx 11$ Hz. Thus, above pH 10, P1 exhibits a coupling constant of 2.1 Hz that corresponds to a dihedral angle of 60−65° or 90−95°, two angles compatible with a short P1−H2 distance. From pH 10−6, the $^3J_{H1-P1}$ couplings increase simultaneously to the protonation fraction increase of P5, reflecting a progressive gain in conformational freedom of phosphate P1. This is in full agreement with the molecular modeling studies which show that the most significant population of rotamers of the deprotonated form A2 is centered on a dihedral angle value of 65° (results not shown).

Interestingly, for compound **4**, where both P4 and P5 are in a cis configuration, the repulsion between the vicinal dianionic phosphates leaves P1 with a large degree of freedom and therefore the H2 wrongway shift is no longer observed. For compounds **2**, **3**, and **4**, the same dynamics take place as described for **1** with a direct effect of the protonation of a phosphate group on a vicinal hydrogen.

Although it must be considered that the conformational and molecular dynamic studies only provide a rough picture of the behavior of the molecules in aqueous medium it can be noted that these studies are fully in line with the observations drawn from the titration experiments. In particular, the conformational freedom of the P1 phosphate is closely related to the protonation degree of P4 and P5, i.e., to the extent of their repulsion.

Beyond the phosphate conformational effect on the equatorial ring protons, the question of the source of both the proton and phosphorus wrongway shifts remains. On the basis of only the ^{31}P NMR titration curves of **1**, the initial deshielding of the P1 resonance was attributed to the formation of a strong hydrogen bond between P1 and OH2.[28,31] By considering the present results, such an explanation no longer holds since the same kind of effect can be observed on phosphates vicinal to a deshydroxylated position where such a bond cannot form. By taking into account these results and previously published observations on nucleotides and nucleic acids,[36,46] it appears that the

(49) Schmitt, L.; Spiess, B.; Schlewer, G. *Bioorg. Med. Chem. Lett.* **1995**, *5*, 1225−1230.

(50) Lindon, J. C.; Baker, D. J.; Farrant, R. D.; Williams, J. M. *Biochem. J.* **1986**, *233*, 275−277.

concomitant ^{31}P and ^{1}H wrongway shift may be the consequence of electrostatic interactions between a ring proton and the doubly negatively charged phosphate group.

How Can Such Interactions Be Termed? According to G. R. Desiraju,[51] who recently addressed some questions related to the now well-established C−H···O hydrogen bonds, the observed interactions may belong to this category. For Desiraju,[51] indeed, "a hydrogen bond is an attractive, directional interaction with certain spectroscopic attributes, structure defining effects, and reproducibility of occurrence." The above-described interactions fulfill these requirements and can be considered as being among the first C−H···O hydrogen bonds reported in aqueous solution.

Clearly, certain conditions are needed for such bonds to form. First, these interactions are favored for a hydrogen and a phosphate group in a trans configuration, albeit cis interactions seem to be tolerated when the C−H position lacks a hydroxyl group as between the axial P4 and the equatorial H3 of **4**. But the most important condition is that the phosphate group and the hydrogen approach at a short distance. This arises when two phosphate groups strongly repel each other upon deprotonation, thus incurring a much shorter distance between the phosphate and the vicinal hydrogen than in the absence of such a constraint. Thus, the conformational studies for **1** showed that the C−H···O distance may be as short as 2.5 Å and the C2−H2−O(P1) angle about 120°, two expected values for weak hydrogen bonding,[51] even though directionality in the C−H···O interaction does not seem to be a necessary condition.[52,53]

It has recently been proposed[54] that hydrogen bonds in aqueous solution may be markedly strengthened by any external factors that enforce their compression. In our case the unusual C−H···O hydrogen bonds result from electrostatic repulsion between two vicinal phosphates leading to a very efficient compression of the C−H···$^{2-}O_3P$−O distance as demonstrated by the molecular modeling studies for compound **1**. The reported results show that the compression effect may be direct on a hydrogen vicinal to a phosphate but may also occur at a longer distance via the bridging role of an equatorial hydroxyl as observed for **1**. In the latter case the effect is less marked, in turn leading to a less marked proton wrongway shift.

The C−H···$^{2-}O_3P$−O interaction may result from a dipole induced on the C−H bond by the highly charged phosphate group approaching at a short distance. Thus, the extent of the wrongway shift and therefore the strength of the hydrogen bond should be correlated, for a given distance, to the basicity of the phosphate group. The limited number of compounds studied does not allow the correlation to be demonstrated, but the few observations made here are consistent with such an assumption.

Conclusion

Biological activities and binding properties of the studied compounds have been performed on various substrates and Ins(1,4,5)P_3 receptors of different tissues.[29,30,55] Although the results are difficult to compare, it can be considered that compounds **2** and **3** bind to the Ins(1,4,5)P_3 receptor about 10-fold less than the natural messenger **1**, and that the difference in binding reaches 3 orders of magnitude between **4** and **1**.[30] This shows that even if the crucial 4,5 bisphosphate/6-hydroxy triad of Ins(1,4,5)P3 is present, as in **2** and **3**, the biological activity is markedly decreased. Such a decrease may be partly due to the subtle interactions and cooperativities between the charged or neutral functional groups driven by small changes in the medium in the immediate environment of the molecules.

Among the interactions to consider, the C−H···O hydrogen bonds, widely invoked in biological crystallography, are also likely to form in solution provided that a highly negatively charged functional group is constrained toward an inositol ring hydrogen. Experimental methods able to characterize such bonds are very scarce and it is necessary to carry out sets of experiments in which one parameter is allowed to vary to follow a dynamic process revealing subtle structural changes. In this regard, multinuclear NMR titrations in an inframolecular approach, as shown in this work, should be of great value.

Acknowledgment. We are grateful to Dr. Y. Chapleur for providing compounds **3** and **4**. We also thank Dr. E. Westhof for fruitful discussion.

JA992940T

(51) Desiraju, G. R. *Acc. Chem. Res.* **1996**, *29*, 441−449.
(52) Novoa, J. J.; Lafuente, P.; Mota, F. *Chem. Phys. Lett.* **1998**, 519−525.
(53) Jeffrey, G. A. *J. Mol. Struct.* **1999**, *485*−*486*, 292−298.
(54) Frey, P. A.; Cleland, W. W. *Bioorg. Chem.* **1998**, *26*, 175−192.
(55) Hirata, M.; Watanabe, Y.; Yoshida, M.; Koga, T.; Ozaki, S. *J. Biol. Chem.* **1993**, *268*, 19260−19266.